

# JOURNAL

## OF THE AMERICAN CHEMICAL SOCIETY

© Copyright 1985 by the American Chemical Society

VOLUME 107, NUMBER 24

NOVEMBER 27, 1985

### Low-Temperature $^{13}\text{C}$ Magnetic Resonance in Solids. 5. Chemical Shielding Anisotropy of the $^{13}\text{CH}_2$ Group<sup>†</sup>

Julio C. Facelli, Anita M. Orendt, Alvin J. Beeler, Mark S. Solum, Gisbert Depke,  
Klaus D. Malsch, John W. Downing, Parvathi S. Murthy, David M. Grant,\* and  
Josef Michl

Contribution from the Department of Chemistry, University of Utah,  
Salt Lake City, Utah 84112. Received June 3, 1985

**Abstract:** The principal values of the  $^{13}\text{CH}_2$  shielding tensors are reported for a series of cycloalkanes, cycloalkenes, and heterocyclic compounds. They were measured on natural abundance samples,  $^{13}\text{C}$ -enriched *tert*-butylcyclohexane-4- $^{13}\text{C}$ , and malononitrile. The assignment of the experimental principal values of the shielding tensor to the molecular frame was based on the results of ab initio IGLO (Individual Gauge for Localized Orbitals) calculations of the shielding tensors. A dipolar experiment in cyclobutane-1,2- $^{13}\text{C}_2$  confirmed the theoretical assignments in this compound. Theoretical and experimental results show good correlation one with another in the variations of the shielding tensor. An empirical correlation of the shift component perpendicular to the CCX plane is found with the CCX angle ( $X = \text{C}, \text{O}, \text{or S}$ ).

The use of very-low-temperature and matrix-isolation techniques in  $^{13}\text{C}$  NMR spectroscopy has proven to be very successful in the study of shielding tensors of small molecules.<sup>1-6</sup> A most serious limitation of the technique is the general lack of information provided by the experimental data on the orientation of the principal axes of the shielding tensor in the molecular frame except in cases of axial symmetry. Otherwise, single crystal, dipolar spectroscopy using doubly labeled materials<sup>4</sup> or 2D experiments<sup>7</sup> are needed to obtain this information. A dipolar study had been done for the  $^{13}\text{CH}_2$  group in cyclopropane,<sup>5</sup> and the orientation of the principal axes in cyclopropane does not correspond to those determined for the  $^{13}\text{CH}_2$  group in a single crystal study of *n*-eicosane.<sup>8</sup> By using the local symmetry axes defined in Figure 1 for the  $^{13}\text{CH}_2$  group, the  $\sigma_{\text{CC}}$  component, which is perpendicular to the CCC plane, is the farthest upfield in cyclopropane and the farthest downfield in *n*-eicosane. The other two components,  $\sigma_{\text{AA}}$ , which bisects the HCH angle, and  $\sigma_{\text{BB}}$ , which is perpendicular to the HCH plane, do not change their relative order, with  $\sigma_{\text{AA}}$  at lower field from  $\sigma_{\text{BB}}$  in both cases. The above observation immediately raises the problem of identifying the relevant electronic and/or geometrical effects that cause the large variation of the  $\sigma_{\text{CC}}$  component, from -36 ppm in cyclopropane to 50.8 ppm in *n*-eicosane. The other two components show a much smaller difference in values;  $\sigma_{\text{AA}}$  changes from 22 to 38.8 ppm and  $\sigma_{\text{BB}}$  from 2 to 17.8 ppm, respectively. The sensitivity of the methylenic shielding tensors to the molecular environment has been recognized in a recent review article.<sup>9</sup>

In this paper the principal values of the  $^{13}\text{CH}_2$  shielding tensors are reported for a series of cycloalkanes, cycloalkenes, and heterocyclic compounds, measured in natural abundance samples and on  $^{13}\text{C}$ -enriched *tert*-butylcyclohexane-4- $^{13}\text{C}$  and malononitrile. Labeled materials were included in this study because preliminary

spectra of cyclohexane indicate that rapid motion persists even at cryogenic temperatures, preventing the observation of the full tensorial pattern. The substitution of an equatorial *tert*-butyl group at the position  $\text{C}_1$  eliminates the averaging motion but requires the use of  $^{13}\text{C}$  at  $\text{C}_4$  in order to obtain a clear tensor pattern. This *tert*-butyl substitution should not affect significantly the tensorial components, and indeed it does not alter the isotropic shielding. Thus, the results reported here are felt to be representative of cyclohexane. Calculations of the shielding tensor in cyclohexane and methylcyclohexane further support this assumption. The labeled malononitrile was available from another independent study.

The problem of assigning the experimental principal values of the shielding tensor to the molecular frame was addressed with measurements on cyclobutane-1,2- $^{13}\text{C}_2$  and with the use of ab initio IGLO (Individual Gauge for Localized Orbitals)<sup>10-13</sup> calculations of the shielding tensors. Previous work<sup>1</sup> has justified the use of

- (1) Beeler, A. J.; Orendt, A. M.; Grant, D. M.; Cutts, P. W.; Michl, J.; Zilm, K. W.; Downing, J. W.; Facelli, J. C.; Schindler, M.; Kutzelnigg, W. *J. Am. Chem. Soc.* **1984**, *106*, 7672.
- (2) Zilm, K. W.; Conlin, R. T.; Grant, D. M.; Michl, J. *J. Am. Chem. Soc.* **1978**, *100*, 8038.
- (3) Zilm, K. W.; Conlin, R. T.; Grant, D. M.; Michl, J. *J. Am. Chem. Soc.* **1980**, *102*, 6672.
- (4) Zilm, K. W.; Grant, D. M. *J. Am. Chem. Soc.* **1981**, *103*, 2913.
- (5) Zilm, K. W.; Beeler, A. J.; Grant, D. M.; Michl, J.; Chou, T. C.; Allred, E. L. *J. Am. Chem. Soc.* **1981**, *103*, 2119.
- (6) Strub, H.; Beeler, A. J.; Grant, D. M.; Michl, J.; Cutts, P.; Zilm, K. W. *J. Am. Chem. Soc.* **1983**, *105*, 3333.
- (7) Linder, M.; Hohener, A.; Ernst, R. R. *J. Chem. Phys.* **1980**, *73*, 4959.
- (8) Vanderhart, D. L. *J. Chem. Phys.* **1976**, *64*, 830.
- (9) Veeman, W. S. *Prog. Nucl. Magn. Reson. Spectrosc.* **1984**, *16*, 193.
- (10) Kutzelnigg, W. *Isr. J. Chem.* **1980**, *19*, 193.
- (11) Schindler, M.; Kutzelnigg, W. *J. Chem. Phys.* **1982**, *76*, 1919.
- (12) Schindler, M.; Kutzelnigg, W. *J. Am. Chem. Soc.* **1983**, *105*, 1360.
- (13) Schindler, M.; Kutzelnigg, W. *Mol. Phys.* **1983**, *48*, 781.

<sup>†</sup> Part 4 of this series: ref 49.

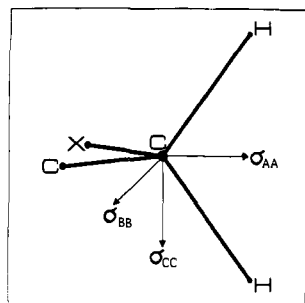


Figure 1. Local symmetry axes for the CH<sub>2</sub> group.

this theoretical method for making tentative but reasonable assignments.

### Experimental and Computational Methods

**Materials.** Research-grade commercial samples of spiropentane, cyclobutane, cyclopentane, ethylene oxide, ethylene sulfide, 1,4-cyclohexadiene, oxetane, cycloheptatriene, 1,4-dioxane, norbornadiene, and tetrahydrofuran were used without further purification. Bicyclo[1.1.1]pentane was synthesized according to the published procedure<sup>14</sup> from 1-(bromomethyl)-3-bromocyclobutane provided by Professor Wiberg (Yale University), bicyclo[1.1.1]pentanone<sup>15</sup> was obtained from Professor Dougherty (California Institute of Technology), and 1,3-cyclopentadiene was distilled from the commercial dimer.<sup>16</sup> The <sup>13</sup>CH<sub>2</sub> enriched malonitrile was provided by Dr. M. T. Chenon (LASIR, Thiais, France).

**4-tert-Butylcyclohexanone-1-<sup>13</sup>C:** A solution of 1,5-dibromo-3-tert-butylpentane<sup>17</sup> (2.7 g) in dry THF (35 mL) was added over a period of 1 h to a stirred suspension of magnesium (1.5 g) in dry THF (6 mL) and kept under nitrogen while the reaction mixture was stirred overnight. The double Grignard reagent was carboxylated by a procedure similar to that of ref 18 by using 1.75 g of Ba<sup>13</sup>CO<sub>3</sub> of 91.6% isotopic purity (Koch Isotopes). After complete addition of carbon dioxide, the reaction mixture was stirred and refluxed overnight. After the usual workup, a pale yellow liquid (0.80 g) was obtained. This product contained 90% of 4-tert-butylcyclohexanone-1-<sup>13</sup>C, as estimated by GC comparison with an authentic sample (QF-1 column); IR (neat) 1710 cm<sup>-1</sup> C=O, 1660 cm<sup>-1</sup> <sup>13</sup>C=O. This material was used as such for further reaction.

**tert-Butylcyclohexane-4-<sup>13</sup>C:** 4-tert-Butylcyclohexanone-1-<sup>13</sup>C (0.8 g) was converted to the *p*-toluenesulfonylhydrazone by refluxing the mixture of the ketone and *p*-toluenesulfonylhydrazide (2.0 g) in methanol (25 mL) for 3 h.<sup>19</sup> After the mixture was cooled in ice, sodium borohydride (2.0 g) was added slowly in small portions. After complete addition, the reaction mixture was refluxed for 3 h, during which time turbidity developed. It was poured into ice-cold water and repeatedly extracted with small quantities of pentane. The combined pentane extracts (15 mL) were washed with water until neutral and then dried over anhydrous sodium sulfate. Pentane was removed with use of a long Vigreux column. The residue contained 80% of tert-butylcyclohexane-4-<sup>13</sup>C (0.30 g) as estimated by GC comparison with an authentic sample. It was purified by preparative GC (50% SP-1200/1.75% Bentone 34 column at 90 °C).

**Cyclobutane-1,2-<sup>13</sup>C<sub>2</sub>:** 1,4-Dibromobutane-1,4-<sup>13</sup>C<sub>2</sub> was prepared starting from 99.0% <sup>13</sup>C potassium cyanide (MSD Isotopes) and 1,2-dibromoethane.<sup>20</sup> The cyclization of the doubly labeled dibromobutane was effected by using a modification of the procedure used in ref 14 to prepare bicyclo[1.1.1]pentane. Lithium amalgam (0.14 g of Li, 28.4 g of Hg) was placed in a flask equipped with a magnetic stirring bar, an addition funnel, a reflux column, and a nitrogen inlet. The lithium amalgam was covered with dry dioxane (10 mL), and the addition funnel was charged with a dioxane (10 mL) solution of 1,4-dibromobutane-1,4-<sup>13</sup>C<sub>2</sub> (1.09 g). The apparatus was attached via the reflux column to a -78 °C trap and a nitrogen bubbler. After the amalgam mixture was heated to reflux, the dibromobutane solution was added dropwise over a 2.5-h period. Heating was continued for an additional 0.5 h, after which the reaction flask was cooled to room temperature. The flow of

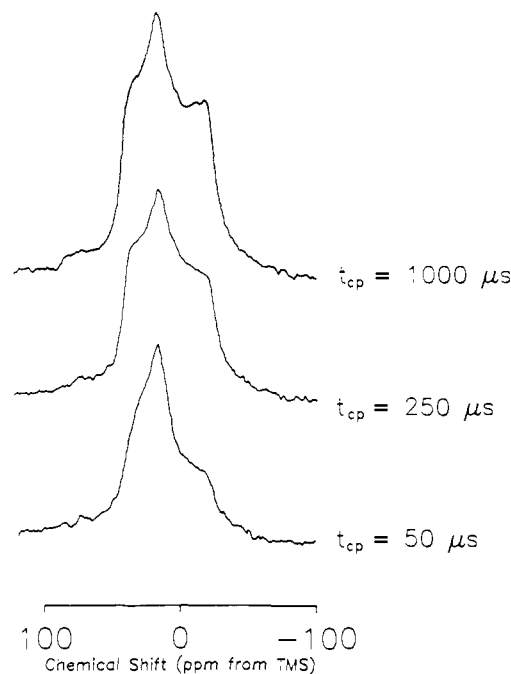


Figure 2. Cross-polarization spectra of spiropentane. The contact time  $t_{cp}$  is defined in Figure 3.

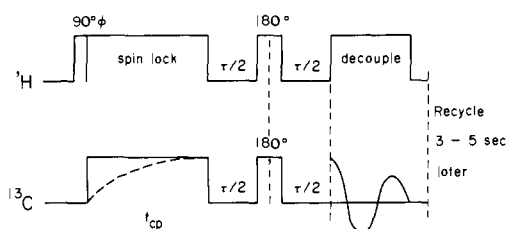


Figure 3. The dipolar dephasing experiment. (See text).

nitrogen was then increased to transfer the product to the cold trap. Transfer to a vacuum line followed by two trap-to-trap distillations (10–20 mtorr) gave 240 mg (83% yield) of pure cyclobutane-1,2-<sup>13</sup>C<sub>2</sub>, which mass spectral analysis showed to be 98% doubly labeled.

In those samples in which a codeposition with Ar was necessary, 99.999% research purity Matheson Gas Co. argon was used. Samples were prepared following the previously described procedures.<sup>21</sup> All chemicals were degassed before deposition with the freeze-pump-thaw technique. Natural abundance samples were prepared neat, except for spiropentane which was measured in a 50% mixture with Ar. The <sup>13</sup>C enriched compounds were measured in a dilution of 0.5% to 2% in Ar to minimize dipolar intermolecular interactions.<sup>4</sup>

**Measurements.** The cryogenic apparatus as well as the home-built spectrometer used in this study have been described previously.<sup>3,21</sup> All spectra were recorded at a temperature of approximately 20 K. The spectrum of the doubly labeled cyclobutane was taken neat at 77 K with a Heli-Tran (Air Products Ltd.) instead of the Displex refrigeration unit; spectra recorded at lower temperatures were more complicated and are currently under investigation. Spectra were recorded at 20.12 MHz with use of the cross polarization method,<sup>22</sup> collecting 10 000 to 15 000 transients. Contact times of about 3 ms and recycle times of 3 to 5 s were used.

For molecules with more than one distinct type of carbon there are often difficulties with overlapping tensor components. In certain cases the individual tensor patterns can be resolved by using variable contact times and dipolar dephasing periods.<sup>23,24</sup> These two techniques have been used with great benefit in the case of spiropentane whose spectrum is shown in Figure 2. For this compound both carbons are aliphatic, and their isotropic shifts differ only by 2.5 ppm, resulting in nearly complete overlap of the two tensorial spectral patterns. Variable contact times,

(14) Wiberg, K. B.; Connor, D. S. *J. Am. Chem. Soc.* **1966**, *88*, 4437.

(15) Sponster, M. B.; Dougherty, D. A. *J. Org. Chem.* **1984**, *49*, 4978.

(16) Rabjohn, N., Ed. "Organic Syntheses"; Wiley: New York, 1963; Collect. Vol. IV.

(17) Johnson, C. R.; McCants, D. Jr. *J. Am. Chem. Soc.* **1965**, *87*, 1109.

(18) Baset, C.; Pichat, L. *Bull. Soc. Chim. Fr.* **1951**, 480.

(19) Cagliotti, L. *Tetrahedron* **1966**, *22*, 487.

(20) Ott, D. G. "Syntheses with Stable Isotopes of Carbon, Nitrogen and Oxygen"; Wiley-Interscience: New York, 1981.

(21) Beeler, A. J. Ph.D. Dissertation, University of Utah, 1984.

(22) Mehring, M. *NMR: Basic Prin. Prog.* **1976**, *11*, 1.

(23) Opella, S. J.; Frey, M. H. *J. Am. Chem. Soc.* **1979**, *101*, 5854.

(24) Alemany, L. B.; Grant, D. M.; Pugmire, R. J.; Alger, T. D.; Zilm, K. W. *J. Am. Chem. Soc.* **1983**, *105*, 2133.

Table I. Experimental and Calculated Principal Values of  $^{13}\text{C}_2$  Shielding Tensors<sup>a</sup>

no.	compound	CCX angle	$\sigma_{AA}$		$\sigma_{BB}$		$\sigma_{CC}$		$\langle \sigma \rangle$		$\sigma_{\text{liq}}$
			exptl	calcd	exptl	calcd	exptl	calcd	exptl	calcd	
I	cyclopropene	49.8	40 <sup>b</sup>	54	29 <sup>b</sup>	13	-59 <sup>b</sup>	-55	3	4	2.3
II	ethylene oxide	59.1	93	74	19	10	19	8	44	31	40.8
III	cyclopropane	60.0	22 <sup>c</sup>	42	2 <sup>c</sup>	-1	-36 <sup>c</sup>	-10	-4	10	-3.8
IV	spiropentane	61.5	37	31	16	-8	-23	-12	10	4	5.9
V	ethylene sulfide	65.8	54	41	7	-8	11	9	24	14	18.7
VI	bicyclo[1.1.1]pentane	73.3	56	59	38	34	54	37	49	43	50.8
VII	bicyclo[1.1.1]pentaone	75.6	87	59	47	29	1	20	45	36	35.6
VIII	cyclobutene	85.8	33 <sup>b</sup>	37	23 <sup>b</sup>	11	43 <sup>b</sup>	60	33	36	31.4
IX	cyclobutane	88.5	23	26	14	-6	39	38	25	19	22.1
X	oxetane C <sub><math>\alpha</math></sub>	91.7	93	69	15	4	104	98	71	57	72.8
	oxetane C <sub><math>\beta</math></sub>	84.6	22	20	4	-10	41	36	22	15	23.1
XI	norbornadiene	96.0	69	66	63	61	97	126	76	84	75.5
XII	tetrahydrofuran C <sub><math>\alpha</math></sub>	109.5	75	57	21	6	110	99	68	54	67.9
	tetrahydrofuran C <sub><math>\beta</math></sub>	105.4	17	-1	17	2	52	50	29	17	25.8
XIII	1,3-cyclopentadiene	102.9	39	40	33	27	51	45	41	37	42.2
XIV	cyclopentane	105.0	21	22	12	4	49	45	27	24	25.3
XV	cyclopentene C <sub><math>\alpha</math></sub>	114.0	30 <sup>b</sup>	29	12 <sup>b</sup>	3	52 <sup>b</sup>	50	31	27	32.8
	cyclopentene C <sub><math>\beta</math></sub>	109.5	22 <sup>b</sup>	18	7 <sup>b</sup>	5	39 <sup>b</sup>	49	23	24	23.3
XVI	1,4-dioxane	109.2	81	62	37	26	86	77	68	55	66.5
XVII	malononitrile	109.4	11	18	-11	-6	30	27	10	13	8.7
XVIII	tert-butylcyclohexane-4- $^{13}\text{C}$ <sup>d</sup>	110.1	57	51	25	20	9	5	30	25	27.0
XIX	1,4-cyclohexadiene	111.9	44	34	21	21	10	8	25	22	25.7
XX	propane <sup>e</sup>	111.9		11		4		17		11	15.9
XXI	1,3,5-cycloheptatriene	113.0	25	28	16	18	55	32	32	26	28.1
XXII	n-eicosane	110.0	39 <sup>f</sup>		18 <sup>f</sup>		51 <sup>f</sup>		36		

<sup>a</sup> Experimental values referenced to Me<sub>4</sub>Si, calculated ones to CH<sub>4</sub> (see the text). The labeling of the principal axes is discussed in the text. <sup>b</sup> From ref 3. <sup>c</sup> From ref 4. <sup>d</sup> Calculated values in C<sub>4</sub> of methylcyclohexane (eq). The calculated values in cyclohexane are  $\sigma_{AA} = 52$ ,  $\sigma_{BB} = 20$ , and  $\sigma_{CC} = 8$  ppm. <sup>e</sup> The experimental spectrum shows an unresolved peak at 16.8 ppm with a half-width of 24 ppm. <sup>f</sup> From ref 8.

$t_{\text{cp}}$ , have been used by CP/MAS workers to characterize the cross-polarization times between carbon and hydrogen. By using small  $t_{\text{cp}}$ 's in spiropentane the powder pattern belonging to the easily polarized CH<sub>2</sub> can be seen without any interference from the quaternary carbon. This is shown in Figure 2 where  $t_{\text{cp}}$  ranges from 50 to 1000  $\mu\text{s}$ . Note that at 50  $\mu\text{s}$  the signal is due almost entirely to the CH<sub>2</sub> carbon, whereas the central carbon signal starts to appear at 250  $\mu\text{s}$  and is fully developed at 1 ms. The timing sequence for the dipolar dephasing experiment is illustrated in Figure 3. It begins like a cross-polarization experiment but after the spins have been fully polarized, the carbon and proton fields are turned off for a time  $\tau/2$  allowing the carbon-proton dipolar interactions to dephase the carbon magnetization. Following the first  $\tau/2$  period a  $\pi$ -pulse is applied in both the carbon and proton channel, refocusing the nondipolar dispersion into an echo after the second  $\tau/2$  delay.  $^{13}\text{C}$  data acquisition is begun at the time of the echo while simultaneously reestablishing the proton-decoupling field. Dephasing times reported in conjunction with CP/MAS experiments<sup>24</sup> are in the range of 40 to 120  $\mu\text{s}$ . In static solids it was found that a  $\tau$  of 40 to 80  $\mu\text{s}$  is sufficient to eliminate any methine or methylene signals. Figure 4 shows the effect of various dephasing times in spiropentane. After 100  $\mu\text{s}$  the signal of the quaternary carbon remains free of any overlapping spectral response due to the CH<sub>2</sub> carbon.

Experimental shieldings are referenced to an external sample of Me<sub>4</sub>Si as described previously.<sup>3</sup> No attempt was made to correct the measurements for bulk susceptibility. The experimental spectra were analyzed either by direct simulation<sup>3</sup> and comparison with the experiment or by using a SIMPLEX fitting method.<sup>25</sup> An error of 2–5 ppm is estimated in the reported values.

**Calculations.** The ab initio calculations were performed with the IGLO method,<sup>10–13</sup> based on the coupled Hartree-Fock perturbation theory with localized molecular orbitals. Huzinaga<sup>26</sup> Gaussian basis sets were used in the calculations as follows: C, (6, 3) contracted to (411, 21) in hydrocarbons and (7, 3) contracted to (4111, 21) in compounds containing heteroatoms; O, (7, 3) contracted to (4111, 21); S, (9, 5) contracted to (411111, 2111); and H, (3) contracted to (2, 1). Geometries used in the calculations were obtained from the following sources: cyclopropane;<sup>27</sup> cyclopropene;<sup>27</sup> ethylene oxide;<sup>27</sup> ethylene sulfide;<sup>27</sup> spiropentane;<sup>27</sup> bicyclo[1.1.1]pentane;<sup>28</sup> bicyclo[1.1.1]pentaone;<sup>15</sup> norbornadiene;<sup>29</sup> cyclobutene;<sup>30</sup> cyclobutane;<sup>31</sup> oxetane;<sup>32</sup> cyclopentane: the

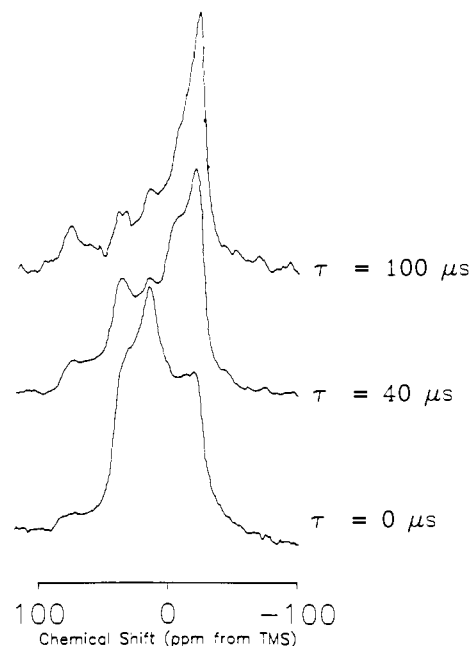


Figure 4. The effect of dipolar dephasing on the spectrum of spiropentane. The dephasing time  $\tau$  is defined in Figure 3.

C<sub>2</sub> structure reported by Adams<sup>33</sup> was assumed for the carbon skeleton, and the HCH angles were taken from the STO-3G optimization given by Wiberg<sup>34</sup>—1,3-cyclopentadiene;<sup>35</sup> cyclopentene;<sup>36</sup> tetrahydrofuran;<sup>37</sup>

(25) Solum, M. S. Ph.D. Dissertation, University of Utah, 1985.  
 (26) Huzinaga, S. "Approximate Atomic Wave Functions"; University of Alberta: Edmonton, Alberta, 1971.  
 (27) Sutton, L. E. "Tables of Interatomic Distances and Configurations of Molecules and Ions"; The Central Society: London, 1958.  
 (28) Chiang, J. F.; Bauer, S. H. *J. Am. Chem. Soc.* **1970**, *92*, 1614.

(29) Yokozeki, A.; Kuchitsu, K. *Bull. Chem. Soc. Jpn.* **1971**, *44*, 2356.  
 (30) Bak, B.; Led, J. J. *J. Mol. Struct.* **1969**, *3*, 379.  
 (31) Skancke, P. N.; Fogarasi, G.; Boggs, J. E. *J. Mol. Struct.* **1980**, *62*, 259.  
 (32) Creswell, R. A. *Mol. Phys.* **1975**, *30*, 217.  
 (33) Adams, W. J.; Geisse, H. J.; Bartell, L. S. *J. Am. Chem. Soc.* **1970**, *92*, 5013.  
 (34) Wiberg, K. B. *J. Am. Chem. Soc.* **1983**, *105*, 1227.  
 (35) Damiani, D.; Ferretti, L.; Gallinella, E. *Chem. Phys. Lett.* **1976**, *37*, 265.  
 (36) Stephenson, D. S.; Binsch, G. *Mol. Phys.* **1981**, *43*, 697.  
 (37) Lambert, J. B.; Papay, J. J.; Akham, S.; Kappauf, K. A.; Magyar, E. S. *J. Am. Chem. Soc.* **1974**, *96*, 6112.

1,4-cyclohexadiene;<sup>38</sup> 1,4-dioxane<sup>39</sup> and cycloheptatriene;<sup>40</sup> malononitrile;<sup>41</sup> and *tert*-butylcyclohexane.<sup>42</sup> cyclopentane. In the last compound a methyl group was substituted for a *tert*-butyl group in the actual calculation, but the ring geometry of *tert*-butylcyclohexane was retained. For comparison with the experimental results, the principal values of the calculated shielding tensor were converted to the Me<sub>4</sub>Si scale assuming that CH<sub>4</sub> and Me<sub>4</sub>Si have the same isotropic chemical shift in gas phase and that both exhibit the same shift going from zero-pressure gas phase to the liquid phase. This assumption is supported by IGLO calculations for CH<sub>4</sub> and Me<sub>4</sub>Si<sup>12</sup> and by the fairly small difference, between 3 and 5 ppm, between their experimental chemical shifts in solution.<sup>43</sup> Absolute shielding values of 211 and 219 ppm were used for CH<sub>4</sub> in the conversion for hydrocarbons and compounds containing heteroatoms, respectively. As the NMR spectra of solids depend only on the symmetric part of the shielding tensor<sup>44</sup> no discussion of the antisymmetric<sup>45</sup> part is presented here. Possible antisymmetric contributions to relaxation times<sup>46,47</sup> are discussed elsewhere.<sup>48</sup> All calculations were performed on a VAX 11/750 computer.

## Results and Discussion

**Principal Values.** In Table I the experimental results as well as the calculated principal values of the shielding tensors are given for compounds I–XXII. The experimental CCX angles (X = C, O, or S) and the liquid chemical shifts are also reported. The assignment of the experimental values in the molecular frame was done by comparison with the calculated shielding tensors, except in cyclopropane,<sup>5</sup> cyclobutane (see below), and *n*-eicosane.<sup>8</sup> Although the assignment of many of the experimental principal values is tentative, a consistent pattern evolves which supports the use of theory to make these assignments, except in those cases where there are large disagreements between experimental and theoretical values or when the presence of two closely calculated values, as in bicyclo[1.1.1]pentane, makes the assignment ambiguous. It is also important to realize that except in those cases in which the local symmetry axes of the <sup>13</sup>CH<sub>2</sub> group (Figure 1) coincide with the symmetry elements of the whole molecule,<sup>45</sup> these local axes do not exactly coincide with the actual principal axes of the tensor. In Table I the principal values are labeled in such a way that for any principal value its principal axis is that closest to the *A*, *B*, or *C* symmetry axes of the <sup>13</sup>CH<sub>2</sub> group. This procedure was adopted in order to facilitate comparisons among the compounds as the angular deviations from the local axes tend to be modest in most molecules lacking the required symmetry elements. The actual orientation of the principal axes in the local <sup>13</sup>CH<sub>2</sub> frame will be discussed later.

The shielding component oriented along the direction which bisects the HCH angle,  $\sigma_{AA}$ , and the one which lies perpendicular to the HCH plane,  $\sigma_{BB}$ , show a narrower range of variation (Table I) than the perpendicular component,  $\sigma_{CC}$ . Significant variations are observed in all three components when the adjacent neighbor is an oxygen atom. The theory reproduces most of the trends observed in Table I. Any theoretical inadequacies are attributed to the limited size of the basis set adopted in the calculations. Previous work has shown a significant improvement in the calculated results when polarization functions are included in the basis set,<sup>1,49</sup> but due to the size of the molecules studied it is not feasible to use such large basis sets in this paper. Other problems in the theoretical work include uncertainties in the molecular geometries and conformations and the inherent problems of the IGLO method (e.g., the neglect of the electron correlation). The

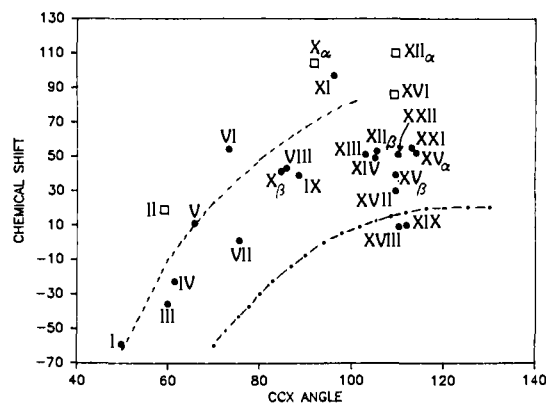


**Figure 5.** Observed  $\sigma_{CC}$  component of the CH<sub>2</sub> shielding tensor as a function of the CCX angle. All values in ppm referenced to Me<sub>4</sub>Si. Compounds numbered as in Table I. Carbons whose first neighbor is an oxygen are designated by squares. Upper and lower dashed lines correspond to the calculated angular dependence of the  $\sigma_{CC}$  component of the chemical shielding of the central <sup>13</sup>C group in symmetrically distorted cyclopropane (---) and propane (---), respectively.

**Table II.** Comparison of the Perpendicular Shielding Component,  $\sigma_{CC}$ , of CH<sub>2</sub> Groups in Cyclopentadiene, 1,4-Cyclohexadiene, and Cycloheptatriene with the Corresponding Values in Aromatic Rings for the Cyclopentadienyl Anion, Benzene, and Tropylium Cation<sup>a</sup>

no. of ring carbons	cycloalkene	aromatic <sup>b</sup>
5	51	21
6	10	9
7	55	22

<sup>a</sup> Experimental values referenced to Me<sub>4</sub>Si. <sup>b</sup> From ref. 6.

full effect of the electronic correlation on the chemical shift has not been adequately studied, but it is expected to be small in hydrocarbons.

Neither the experimental nor the calculated values show any dependence of the  $\sigma_{AA}$  and  $\sigma_{BB}$  components upon either the CCX bond angles or the size of the ring.

The  $\sigma_{CC}$  component which lies perpendicular to the CCX plane shows a very different behavior. It moves from -59 ppm in cyclopropane to 110 ppm for the  $\alpha$ -carbons of tetrahydrofuran. The data in Table I and Figure 5 support the theoretical finding that  $\sigma_{CC}$  is correlated with the CCX angle. In Figure 5, the experimental values of  $\sigma_{CC}$  plotted against the CCX angle largely fall between the two dashed lines which show the theoretical angular dependence of the  $\sigma_{CC}$  component of the central methylene group in symmetrically distorted cyclopropane and propane. In the former case, only relatively small CCC angles were considered since the single determinant representation of the ground-state wave function becomes unphysical at large values of this angle. A smooth angular dependence is obtained in both calculations, while the experimental values are scattered largely between these two curves, approaching the cyclopropane curve at smaller angles and the propane curve at larger angles as one might expect. It is obvious from the general scatter and from a few prominent deviations that additional electronic effects are superimposed on the geometrical effect associated with the CCX angle. This is also apparent from the fact that the curves in the model compounds do not coincide. The presence of an electronegative atom, such as oxygen, shifts the  $\sigma_{CC}$  component to lower fields. Electronegativity effects are well known in isotropic shifts, and here the effect is manifested in the  $\sigma_{CC}$  component. Electronegativity effects are also observed in the other two components to varying degrees. Unfortunately, the experimental  $\sigma_{CC}$  value for propane is still unavailable. However, the calculated values are consistent with the experimental spectrum, which shows an unresolved peak at 16.8 ppm with a half-width of 24 ppm.

The theory reproduces most of the observed effects in the  $\sigma_{CC}$  component. Theoretical results suggest that the crossover of the perpendicular component in its movement downfield with increasing CCX angles occurs at an angle of 65 to 80°. This

(38) Oberhammer, H.; Bauer, S. H. *J. Am. Chem. Soc.* **1969**, *91*, 10.

(39) Davis, M.; Hassel, O. *Acta Chem. Scand.* **1963**, *17*, 1181.

(40) Traetteberg, M. *J. Am. Chem. Soc.* **1964**, *86*, 4265.

(41) Hirota, E.; Morino, Y. *Bull. Chem. Soc. Jpn.* **1960**, *33*, 705.

(42) Altona, C.; Sundaralingam, M. *Tetrahedron* **1970**, *26*, 925.

(43) Jackowski, K.; Raynes, W. T. *Mol. Phys.* **1977**, *34*, 465.

(44) Griffin, R. G.; Ellett, J. D.; Mehring, M.; Bullitt, J. G.; Waugh, J. S. *J. Chem. Phys.* **1972**, *57*, 2147.

(45) Buckingham, A. D.; Malm, S. M. *Mol. Phys.* **1971**, *22*, 1127.

(46) Spiess, H. W. *NMR: Basic Prin. Prog.* **1978**, *15*, 55.

(47) Iwai, M.; Saika, A. *Chem. Phys. Lett.* **1983**, *95*, 596.

(48) Facelli, J. C.; Orendt, A. M.; Grant, D. M.; Michl, J. *Chem. Phys. Lett.* **1984**, *122*, 147.

(49) Orendt, A. M.; Facelli, J. C.; Grant, D. M.; Michl, J.; Walker, F. H.; Dailey, W. P.; Waddell, S. T.; Wiberg, K. B.; Schindler, M.; Kutzelnigg, W. *Theor. Chim. Acta*, in press.

**Table III.** Calculated Angles between the  $\sigma_{AA}$  Component of the Shielding Tensor and the Bisector of the HCH Angle<sup>a</sup>

no.	compound	$\delta$ (deg)
II	ethylene oxide	15.9
IV	spiropentane	8.7
V	ethylene sulfide	5.5
VIII	cyclobutene	6.9
X	oxethane $C_\alpha$	26.6

<sup>a</sup>The angle  $\delta$  is defined in Figure 6.

conclusion is supported by the results for doubly labeled cyclopropane and cyclobutane which bracket the crossover point. The limited number of experimental measurements in this angular range as well as the uncertainties introduced by electronegativity effects discussed above prevent us from establishing a precise experimental value for the crossover point. Furthermore, the theory predicts exceptions to this rule in two of the six-membered ring compounds, 1,4-cyclohexadiene and *tert*-butylcyclohexane, in which the  $\sigma_{CC}$  component appears farthest upfield. The behavior of the  $\sigma_{CC}$  component in these six-membered ring compounds closely resembles the trend found for the perpendicular component of aromatic five-, six-, and seven-membered rings.<sup>6</sup> In Table II the  $\sigma_{CC}$  shieldings in cyclopentadiene, 1,4-cyclohexadiene, and cycloheptatriene are compared with those of the perpendicular component in the cyclopentadienyl anion, benzene, and the tropylium cation. The greater variation observed in the methylene carbons is in agreement with the general trend found in this laboratory: specific components of the shielding tensors of saturated carbons tend to be more dependent on the molecular environment than those of unsaturated or aromatic carbons, which, however, generally exhibit much greater overall anisotropy.

It is important to point out that exceptions to the trends contained in Figure 5 have been found in the  $\text{CH}_2$  shielding tensors of bicyclo[1.1.0]butane and [1.1.1]propellane;<sup>49</sup> this may be caused by the unusual electronic structure of these highly strained molecules.

**Calculated Principal Axes of the Shielding Tensors.** To determine completely the symmetric part of the shielding tensor in a specific molecular frame, in the most general case it is necessary to give the three principal values and the direction cosines or Euler angles which define the orientation of these principal axes. In the following, the local  $^{13}\text{CH}_2$  symmetry axes (Figure 1) are used as the molecular frame. The actual number of parameters necessary to describe completely the shielding tensor can be reduced by the symmetry of the molecule.<sup>45</sup> Symmetry planes which contain the nucleus under consideration require the normal to the plane to be a principal axis of the shielding tensor. This is the case in an isolated  $^{13}\text{CH}_2$  group, in which all the principal axes, *A*, *B*, and *C* (Figure 1), are determined by symmetry. For compounds I, III, VI, X( $C_\beta$ ), XI, XIII, XVII, and XX the local symmetry elements of the entire molecule coincide with those of the  $^{13}\text{CH}_2$  group and, therefore, the orientation of the principal axes of the shielding tensor is determined by symmetry. In all the other compounds considered in this paper, at least one of the local  $^{13}\text{CH}_2$  symmetry planes is not simultaneously a symmetry plane of the molecule. In the absence of single crystal or dipolar studies only theory provides a complete description of the shielding tensor. Even the information obtained from studies on doubly labeled compounds may be insufficient due to the  $C_\infty$  symmetry of the dipolar interaction. One symmetry plane provides sufficient additional information to make unequivocal assignments, provided the angle of the dipolar vector relative to the symmetry plane is known and not equal to 0, 45, or 90°.

In compounds, II, IV, V, VIII, and X( $C_\alpha$ ) the CCX plane is a symmetry plane of the molecule and, therefore, the axis perpendicular to this plane is a principal axis of the shielding tensor with the principal values  $\sigma_{CC}$ . The components  $\sigma_{AA}$  and  $\sigma_{BB}$  lie in the CCX plane, but they are rotated from the local symmetry axes by an angle  $\delta$  away from the  $^{13}\text{CH}_2\text{-CH}_2$  bond (Figure 6). The calculated values of the  $\delta$  angle are given in Table III.

In the nonplanar compounds VII, IX, XIV ( $C_s$  symmetry was assumed), XV( $C_\beta$ ), XVIII, XIX, and XXI the direction bisecting

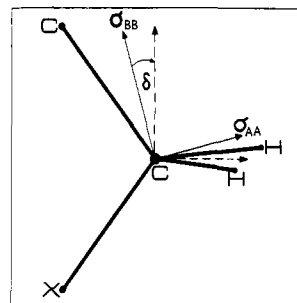


**Figure 6.** Description of the rotation angle  $\delta$ , around the C axis, used to define the orientation of the shielding tensor principal axes in the local symmetry  $^{13}\text{CH}_2$  axes in compounds II, IV, V, and VIII (X = O, S, or C).

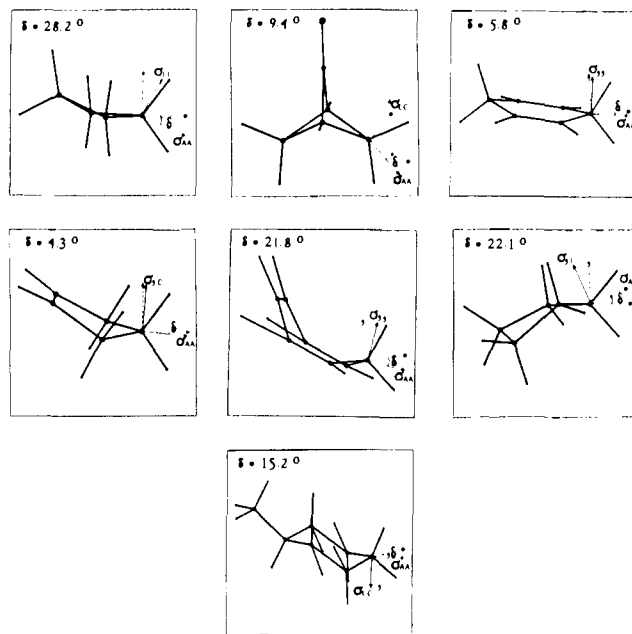


**Figure 7.** Calculated angles between the  $\sigma_{AA}$  component of the shielding tensor and the direction bisecting the HCH angle. Rotations are around the *B* axis.

the HCH angle and the one perpendicular to the CCC plane are no longer principal axes of the shielding tensor, but the direction perpendicular to the HCH plane is a principal axis with eigenvalue  $\sigma_{BB}$ . The orientations of the  $\sigma_{AA}$  and  $\sigma_{CC}$  components in the HCH plane are reported in Figure 7. The calculated IGLO values of the rotation around the *B* axis are also given.

The SIMPLEX fitting<sup>25</sup> of the cyclobutane-1,2- $^{13}\text{C}_2$  spectrum was performed in order to obtain the orientation of the shielding tensor relative to the dipolar axis. The best SIMPLEX fit places the upfield component perpendicular to the HCH plane,  $\sigma_{BB}$ , and the downfield and middle components in the HCH plane. The downfield component lies at 77.9° from the dipolar axis and, therefore, is associated with  $\sigma_{CC}$ . The middle component is assigned to  $\sigma_{AA}$  as it lies at an angle of 8.6° from the HCH bisector. This assumes a CCC angle of 88.5° and no rocking of the methylene group. These experimental assignments agree well with the calculated orientation, where the angle between  $\sigma_{CC}$  and the dipolar axis is 70.2° and the angle off the HCH bisector angle is 28.2°. The experimental spectrum and the one simulated by using the best SIMPLEX parameters are shown in Figure 8.

Due to the lack of symmetry in compounds XII, XIV, and XV( $C_\alpha$ ) it is convenient to give the direction cosines between axes of the shielding tensor and the local  $^{13}\text{CH}_2$  symmetry axes to describe the shielding tensor completely. This information is given in Table IV where the principal shielding axes are denoted by Greek letters.

With minor exceptions the deviation of the principal axes of the shielding tensor from the local symmetry axes is small (4 to

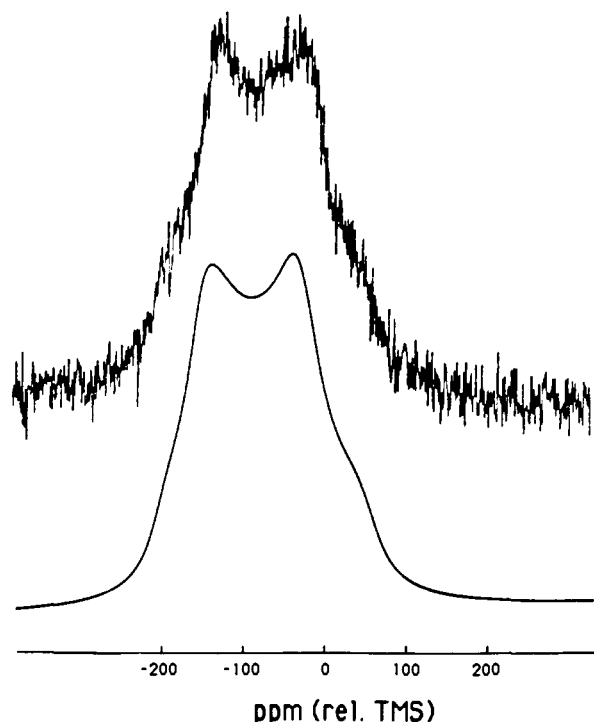


**Figure 8.** Comparison of experimental and simulated dipolar spectra of cyclobutane-1,2- $^{13}\text{C}_2$ .

**Table IV.** Calculated Direction Cosines between the Local  $\text{CH}_2$  Axes and the Principal Axes of the Shielding Tensor<sup>a</sup>

	A	B	C	eigenvalues <sup>b</sup>	
				calcd	exptl
Cyclopentene $\text{C}_\alpha$					
$\alpha$	0.9597	0.0449	0.2774	29	30
$\beta$	-0.0202	-0.9735	-0.2778	3	12
$\gamma$	0.2803	-0.2242	-0.9334	50	52
Tetrahydrofuran $\text{C}_\alpha$					
$\alpha$	-0.8575	-0.5027	-0.1092	57	76
$\beta$	0.5061	0.8625	0.0039	6	24
$\gamma$	0.0923	-0.0587	0.9940	99	110
Tetrahydrofuran $\text{C}_\beta$					
$\alpha$	-0.8394	0.5319	-0.1121	-1	16
$\beta$	-0.5418	-0.8354	0.0933	2	19
$\gamma$	-0.0439	-0.1391	0.9893	50	53
1,4-Dioxane					
$\alpha$	-0.9100	-0.3464	0.2279	62	82
$\beta$	0.2532	-0.8995	-0.3561	26	37
$\gamma$	0.3284	-0.2663	0.9062	77	86

<sup>a</sup> A, B, and C denote the  $\text{CH}_2$  local symmetry axes, and  $\alpha$ ,  $\beta$ , and  $\gamma$  denote the principal axes of the shielding tensor. <sup>b</sup> Experimental values referenced to  $\text{Me}_4\text{Si}$ , calculated ones to  $\text{CH}_4$  (see the text).

35°), showing that the principal axes are primarily determined by the local  $\text{CH}_2$  symmetry.

**Shifts of Other Carbon Atoms.** For the sake of completeness some of the chemical shift tensors obtained in groups other than methylene are also listed. Methine tensors will be reported in the following paper of this series.<sup>50</sup> Spiro carbon in spiropentane  $\sigma_{11}$

= 81 ppm,  $\sigma_{22} = \sigma_{33} = -24$  ppm;  $\text{C}_{2,3,5,6}$  in norbornadiene  $\sigma_{11} = 259$  ppm,  $\sigma_{22} = 130$  ppm,  $\sigma_{33} = 40$  ppm; 1,3-cyclopentadiene ( $\text{C}_\alpha$ )  $\sigma_{11} = 227$  ppm,  $\sigma_{22} = 130$  ppm,  $\sigma_{33} = 39$  ppm, ( $\text{C}_\beta$ )  $\sigma_{11} = 227$  ppm,  $\sigma_{22} = 136$  ppm,  $\sigma_{33} = 39$  ppm;  $\text{C}_{1,2,4,5}$  in 1,4-cyclohexadiene  $\sigma_{11} = 235$  ppm,  $\sigma_{22} = 119$  ppm,  $\sigma_{33} = 19$  ppm; carbonyl carbon in bicyclo[1.1.1]pentanone  $\sigma_{11} = 295$  ppm,  $\sigma_{22} = 154$  ppm,  $\sigma_{33} = 106$  ppm.

### Conclusion

With the growing collection of shielding tensor components for related molecular systems, systematic trends and correlations are beginning to emerge. The correlation between the in-plane angle and the value of the highly variable methylene shift component perpendicular to the  $\text{CCX}$  plane clearly exhibits the sensitivity of the methylenic chemical shielding to geometrical structure. The large upfield isotropic chemical shift of three-membered rings has now been related to the behavior of a single component, the  $\sigma_{\text{CC}}$  component.

The rapid accumulation of well-characterized shielding tensors is seriously curtailed, however, by the general unavailability of experimentally determined tensorial values and the orientation of their principal axes. Fortunately, for small enough molecules quantum chemical calculations of  $^{13}\text{C}$  shielding tensors have been sufficiently reliable in cases where the orientations are already known that it now appears one is justified in using theory to make tentative assignments of the shielding principal axes to the experimentally determined principal values. This has been done in all cases except those in which the principal values are quite close together. The consistency between the experimental and theoretical results obtained in this paper continues to support this conclusion. Theory also provides information on the orientation of the shielding tensor in the molecular frame. Except in a few cases, the data on methylene shieldings indicate that the local  $\text{C}_{2v}$  symmetry of the  $\text{CH}_2$  group appears to dominate the orientation of the principal axes of the shielding tensor. Electronic effects other than those associated with the geometric angles were found to alter both the shielding values and the orientations, but sufficient information is unavailable to discuss these features in any detail at the present time.

**Acknowledgment.** This work was supported by the National Science Foundation under Grant CHE 83-10109. Acknowledgment is made to the donors of the Petroleum Research Fund, administered by the American Chemical Society, for the support of this research (PRF 13172-AC4,6). The authors are grateful to Drs. W. Kutzelnigg and M. Schindler for the copy of their IGLO program and to Drs. M. T. Chenon, D. A. Dougherty, and K. B. Wiberg for providing us with some of the compounds used in this study. K.D.M. was partially supported by the A.v.H. Foundation.

**Registry No.** I, 2781-85-3; II, 75-21-8; III, 75-19-4; IV, 157-40-4; V, 420-12-2; VI, 311-75-1; VII, 93061-30-4; VIII, 822-35-5; IX, 287-23-0; X, 503-30-0; XI, 121-46-0; XII, 109-99-9; XIII, 542-92-7; XIV, 287-92-3; XV, 142-29-0; XVI, 123-91-1; XVII, 109-77-3; XVIII, 98760-44-2; XIX, 628-41-1; XX, 74-98-6; XXI, 544-25-2; 4-*tert*-butylcyclohexanone-1- $^{13}\text{C}$ , 98760-45-3; 1,3-dibromo-5-*tert*-butylpentane, 98760-46-4; 1,4-dibromobutane-1,4- $^{13}\text{C}_2$ , 79341-54-1; cyclobutane-1,2- $^{13}\text{C}_2$ , 98760-47-5.

(50) Facelli, J. C.; Orendt, A. M.; Solum, M.; Grant, D. M.; Michl, J., manuscript in preparation.